

Tight Binding Molecular Dynamics Studies of Boron Assisted Nanotube Growth

E. Hernández * and P. Ordejón

Institut de Ciència de Materials de Barcelona - CSIC, Campus de la Universitat Autònoma de Barcelona, 08193 Bellaterra, Barcelona, Spain

I. Boustani

Bergische Universität - Gesamthochschule Wuppertal, FB 9 - Theoretische Chemie, Gaußstraße 20, D-42097 Wuppertal, Germany

A. Rubio and J.A. Alonso

Departamento de Física Teórica, Universidad de Valladolid, 47011 Valladolid, Spain
(October 26, 2018)

In this paper we report a theoretical study of the effects of the presence of boron in growing carbon nanotubes. We employ a well established Tight Binding model to describe the interactions responsible for the energetics of these systems, combined with the Molecular Dynamics simulation technique and Structural Relaxation calculations. We find, in agreement with the previous theoretical/experimental work of Blase *et al.* [*Phys. Rev. Lett.* **83**, 5078 (1999)], that boron favors (n,0) (zig-zag) tubular structures over (n,n) (arm-chair) ones by stabilizing the zig-zag edge. Furthermore, it is shown that boron has the effect of delaying the tube closure process, a fact which could explain the improved aspect ratio experimentally observed in nanotubes synthesized in the presence of boron. Our dynamical simulations lead us to propose a mechanism through which this extension of the closure time can be explained.

I. INTRODUCTION

The discovery of carbon nanotubes by Iijima in 1991¹ has marked the starting point of a scientific revolution²⁻⁶. This discovery has opened a whole new perspective in the nanoscopic regime of Materials Science and Engineering. Their mechanical⁷⁻¹⁴, electrical^{15,16} and magnetic¹⁷⁻¹⁹ properties provide ample opportunity for the fabrication of nano-scale devices. Indeed some such devices have already been reported in the literature²⁰⁻²³. Since Iijima's, discovery nanotubes of other chemical composition have also been synthesized, such as $B_xC_yN_z$ composite nanotubes²⁴⁻²⁸, the so-called inorganic nanotubes consisting of layers of MoS_2 or WS_2 ²⁹⁻³¹, or $NiCl_2$ nanotubes³². All these compounds have phases which consist of layered structures, and this has lead to the prediction that other materials also capable of crystallizing in layered structures can in principle produce nanotubes. Indeed, theoretical arguments have been presented in the literature for the viability of BN ^{33,34}, BC_3 ³⁵, BC_2N ³⁶, GaN ³⁷, B^{38} , $GaSe$ ³⁹ and P^{40} nanotubes. Interestingly, nanotubular structures can also be constructed from biochemical compounds, such as peptides, as demonstrated experimentally by Ghadiri *et al.*⁴¹ and theoretically by Carloni *et al.*⁴².

The tubes first detected by Iijima¹ were multi-wall nanotubes (MWCNT's), *i.e.* concentric shells of cylindrical shape, in which each shell is separated from the next by approximately the same distance as the inter-layer spacing in graphite. Each shell can be characterized by a pair of indices, (n,m), which determine how the folding of the graphene sheet must be carried out in or-

der to obtain the shell. The shells are usually classified into three different types: (n,0) or *zig-zag* shells, (n,n) or *arm-chair* shells, and *chiral* shells, of indices (n,m) where $n > m > 0$. Zig-zag and arm-chair shells are said to be achiral (they can be superimposed onto their mirror images). The ordering of the shells in a MWCNT is usually *turbostratic*, *i.e.* the pattern of atomic arrangement may vary (and in general does vary) from one shell to the next, or in other words, different shells usually have different chiralities⁴.

After the discovery of MWCNT's, a procedure for synthesizing single-wall nanotubes (SWCNT's) was found⁴³. These tubes are found to aggregate into bundles or ropes, and their diameter distribution peaks at around 1.4 nm, although more recently this distribution has been found to vary according to the synthesis conditions⁴⁴. The production of SWNT's has allowed the experimental corroboration¹⁶ of a theoretical prediction made by Hamada and coworkers¹⁵ soon after the discovery of MWCNT's, that the electrical conductivity properties of SWCNT's are dependent on the (n,m) indices. This prediction stated that SWCNT's can be either metallic or semi-conducting; if the indices (n,m) of a nanotube obey the relation $n - m = 3q$ ($q = 0, 1, 2, 3, \dots$), then the tube is metallic, otherwise the tube is semi-conducting. This dependence of the electric characteristics of SWCNT's upon their structure has raised an interest in the possibility of devising new synthetic methods that allowed a structural selection of nanotubes, not only according to their diameter, but also to their chirality. A first step in this direction was achieved by Redlich *et al.*⁴⁵, Carroll *et al.*⁴⁶, and by Terrones *et al.*⁴⁷, who, by adding a certain

amount of boron during the synthesis, obtained boron doped MWCNT's which, interestingly, have an improved crystallinity and a larger aspect ratio (quotient of length to diameter) with respect to tubes obtained in the absence of boron. It was shown that boron appears mostly in the form of clusters associated with the tips of the nanotubes. But most importantly, a recent combined experimental and theoretical study by Blase and coworkers⁴⁸ has demonstrated that the MWCNT's thus obtained consist mostly of zig-zag shells. This study also sheds some light on the role played by boron in favoring the zig-zag structure over others, and tries to explain the larger aspect ratio observed in boron assisted synthesis. This latter issue, though, was addressed by First-Principles (FP) Density Functional Theory (DFT) Molecular Dynamics simulations, and the large computational costs of this technique prevented Blase and coworkers from pursuing a detailed enough study which clarified completely this question.

In this paper we address the problem of boron assisted nanotube growth using a Tight Binding model⁴⁹. Tight Binding (TB) is an approximate method which nevertheless is capable of providing extremely accurate results in favorable systems. Its main advantage with respect to FP methodologies is its comparatively low computational cost, which often allows a more extensive study than is practical or even possible with higher levels of theory. In this work we have used the Density-Functional Tight Binding (DFTB) model due to Porezag *et al*⁵⁰, about which we give more details in Section II. This model has proved to be very accurate for carbon based systems. We have used DFTB to perform a series of static and dynamical simulations of SWCNT's, with and without boron present, with the aim of understanding the effects of the presence of boron on the structural properties of the resulting NT's. The structure of this paper is as follows: in Section II we describe briefly the DFTB model, and provide previous examples of its successes in order to justify its use here. We also describe the calculations which are reported in the remaining of the paper. Section III is devoted to a discussion of our simulation results, and we summarize our conclusions in Section IV.

II. COMPUTATIONAL DETAILS

A. Model

DFTB is a non-orthogonal Tight Binding scheme in which a parametrisation is constructed directly from DFT calculations using atomic-like orbitals in the basis set, and adopting a two-center approximation for the Hamiltonian matrix elements. For more details on the parametrisation used here the reader should consult references^{50,51}. The DFTB scheme has proved to be extremely successful in the modeling of carbon-based systems, in particular carbon clusters and nanostructures.

Fowler *et al.*⁵² have used it to analyze the energetic ordering of all 426 cage structures containing 5, 6 and 7-membered rings in C₄₀. Ayuela *et al.*⁵³ have found, using DFTB and other five semi-empirical methods, a heptagon-containing isomer of C₆₂ which was predicted to be more stable than any of the other 2385 classical fullerene isomers (*i.e.* isomers containing only pentagons and hexagons). DFTB has also been used to determine the mechanical properties of single-wall C, BN and some B_xC_yN_z nanotubes¹¹, providing results which are in excellent agreement with the available experimental data. More recently DFTB has also been used to study the structural, mechanical and electronic properties of a novel family of laminar carbon structures known as *Haeckelites*, as well as those of their tubular counterparts⁵⁴. Haeckelites consist of pentagons and heptagons in equal number, with an arbitrary number of hexagons. The suitability of DFTB for performing Molecular Dynamics simulations in carbon-based systems has been most recently demonstrated by Fugaciu *et al.*⁵⁵, who have used it to study the conversion of diamond nanoparticles to concentric shell fullerenes. The many examples of the use of DFTB in the context of carbon based systems and the accuracy of the results reported give us confidence in the reliability of this theoretical model.

Like in other Tight Binding models⁴⁹, in DFTB the total energy is calculated as the sum of two contributions: the *band structure* contribution, which is mostly attractive, and the repulsive *pair-potential* contribution, which accounts for the core-core repulsion and the double-counting of the electron-electron interaction which is implicit in the band structure term. The band structure energy is calculated by straight forward diagonalisation of the Hamiltonian, summing the eigen-values of the occupied states weighted according to their occupation numbers, *i.e.*

$$E_{bs} = 2 \sum_n f_n \epsilon_n, \quad (1)$$

where f_n is the population of state n (which in our case is equal to 1 for occupied states, and to zero for unoccupied, *i.e.* we have assumed 0 K electronic temperature), and ϵ_n is the eigen-value of state n . The factor of two accounts for the degeneracy of spin. The band structure contribution to the atomic force \mathbf{F}_i is then calculated from the Hellmann-Feynman theorem:

$$\nabla_i \epsilon_n = 2 f_n \mathbf{C}_n^\dagger (\nabla_i \mathbf{H} - \epsilon_n \nabla_i \mathbf{S}) \mathbf{C}_n, \quad (2)$$

where \mathbf{C}_n is the vector representation of eigen-state n , \mathbf{H} is the Hamiltonian matrix, and \mathbf{S} is the overlap. The repulsive pair potential energy and force contributions are trivially added to equations 1 and 2, respectively.

B. Calculations

We have performed two types of calculations: a) structural relaxation calculations, in which, using the Conjugate Gradients (CG) technique⁵⁶, the positions of the atoms in a system are displaced until a minimum in the potential energy hyper-surface is found; and b) molecular dynamics (MD) simulations, which we have employed to study the time evolution of the systems considered here at a range of temperatures. More specifically we have performed canonical ensemble molecular dynamics calculations, in which the conserved quantities are the number of atoms, the volume and the average temperature (NVT-MD). We have implemented the NVT-MD algorithm of Nosé as modified by Hoover^{57,58}. In this algorithm the physical system of interest is extended by the addition of an extra degree of freedom, playing the role of a thermostat, which interacts with the physical system in such a way as to fix the average temperature. In this algorithm the mass associated with the thermostat is somewhat arbitrary, as it does not affect the value of the average temperature, only the size of the instantaneous temperature fluctuations. We have chosen this mass to be equal to the total mass of the physical system. We have used the implementation of the Nosé-Hoover algorithm described by Frenkel and Smit⁵⁹. Although the total energy is not conserved in NVT-MD, there is a conserved quantity which can be monitored to ensure the correctness of the implementation. This magnitude plays the role of total energy of the extended system. In our simulations we have used a time-step of 1 fs, which has proved to be sufficiently small to maintain the conserved quantity oscillations smaller than 1 part in 10000 during the length of the simulations, with no appreciable drift.

Our studies have covered a range of temperatures, namely 1000, 2000, 2500 and 3000 K. At each temperature the dynamics of the system were monitored during at least 10 ps. The simulations were carried out sequentially, using the coordinates and velocities at the end of a run at a given temperature as a seed for the simulation at the next higher temperature. The transition from one temperature to another was made by gradually increasing the temperature of the thermostat at a rate of 0.5 K/fs. To use a lower heating rate would be prohibitive, in view of the computational costs involved. Nevertheless, once the thermostat reached the desired temperature, the system was allowed to reach equilibrium at the new temperature during 1 ps, in order to minimize as much as possible the effects of such a high heating rate, before performing the simulation at the new temperature.

III. SIMULATION RESULTS

A. Carbon nanotubes in the absence of boron

Before addressing the effect of boron on the structure and growth mechanism of nanotubes, it is necessary to study the dynamics of carbon nanotubes in the absence of boron. In so doing we can also assess the quality and appropriateness of the model. In order to study the dynamics of the open ended tubes, we first considered the systems illustrated in Figure 1. These systems are a (10,0) nanotube, with one end saturated by ten H atoms, and a (5,5) nanotube, also with one end saturated by ten H atoms. Both tubes consist of 120 C atoms, plus the 10 H atoms. Figure 1 shows the structures obtained after a CG relaxation, which were then used as starting configurations for the NVT-MD simulations. To facilitate the analysis of the MD simulations, the 10 H atoms were kept fixed throughout the dynamical simulations. While this is an approximation, we have chosen a tube section as large as was practical in order to minimise the possible effects of having the H atoms frozen on the dynamics at the other end of the tube.

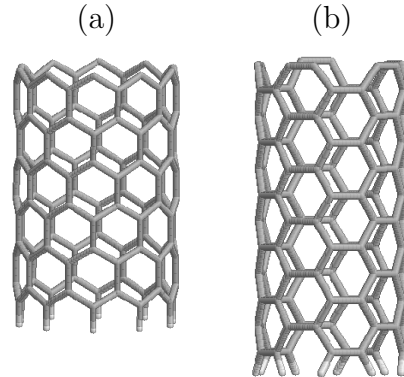


FIG. 1. The relaxed structures of a (10,0) nanotube (a) and a (5,5) nanotube (b), used as starting configurations for the Molecular Dynamics simulations described in the text.

We first discuss the case of the (10,0) nanotube. At the lowest temperature considered (1000 K) the structure of the nanotube remains unaltered except for the normal thermal oscillations around the equilibrium atomic positions. All the hexagonal rings present in the initial structure (Figure 1) retain their identity, as can be seen in Figure 2(a), which illustrates the configuration attained after 10 ps of MD run at this temperature. In view of the fact that the simulation of the open nanotube end at 1000 K failed to produce any structural reordering within this time scale, we proceeded to heat the system up to 2000 K. At this temperature, structural changes begin to appear in the open edges of the nanotube, as can be seen in Figure 2(b). Indeed, some hexagonal rings at the edge have been broken, resulting in chains of carbon atoms, while others have fused into pentagon-heptagon (5/7) pairs. After 10 ps at 2000 K, two pentagonal rings can be seen, as well as one heptagon. These non-hexagonal rings are produced by the fusing of two hexagons, to give a pen-

tagon and a heptagon. However, we find that heptagons appear to be less stable, and break more easily into carbon chains that remain attached to the nanotube edge, while the pentagons remain stable. The presence of these pentagons induces curvature in the structure, so the edge of the nanotube bends inwards.

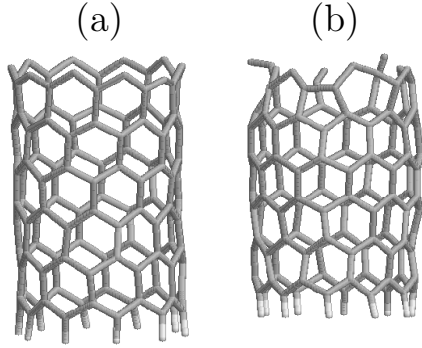
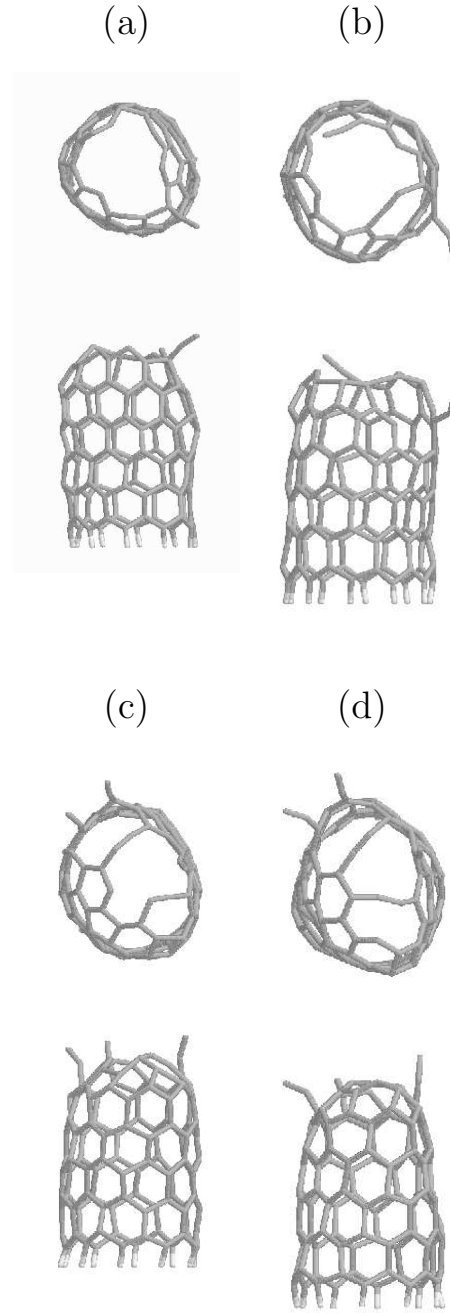


FIG. 2. (a) Final structure of the (10,0) nanotube obtained after 10 ps of dynamics at 1000 K. (b) Final structure of the (10,0) nanotube obtained after 10 ps of dynamics at 2000 K.

Clearly, a tendency to form a fullerene-like cap is observed, a situation that is after all energetically more stable than the open edge. Therefore, we continued the simulation at a temperature of 2500 K. Like before, the temperature of the thermostat was increased at a rate of 0.5 K/fs, and once the desired thermostat temperature was achieved the combined system of nanotube and thermostat was allowed to equilibrate during 1 ps. The dynamics of the system were then monitored during a further 20 ps. Figure 3 illustrates six representative configurations of the system at this temperature. As can be seen, the process of tube closure initiated at 2000 K is further facilitated at 2500 K. The chains of carbon atoms which were seen already at 2000 K can now form links bridging across the open edge. This, combined with the presence of the pentagonal rings at or close to the edge, has the overall effect of bending inwards the nanotube walls. As the simulation proceeds, the number of freely oscillating chains is reduced, due to their tendency to bond into the dome-like structure being formed. Eventually the tube closure is completed, and all carbon atoms are three-coordinated in an sp^2 hybridisation fashion. Although the resulting closed structure is highly strained, due to the presence of some small rings (a tetragon can be seen) and to the adjacency of pentagons, this is certainly a deep local minimum of the potential energy hypersurface, as the structure, once closed, remains unaltered (except for thermal oscillations), even after heating up the system to 3000 K and following the dynamics at this temperature for a further 10 ps. Obviously, the time-scale for structural re-orderings once the nanotube has closed is much larger than the time-scale for the closure itself. This is because structural changes now must happen via the Stone-Wales⁶⁰ mechanism, which has a high activation barrier, and therefore occurs very infrequently⁶¹.



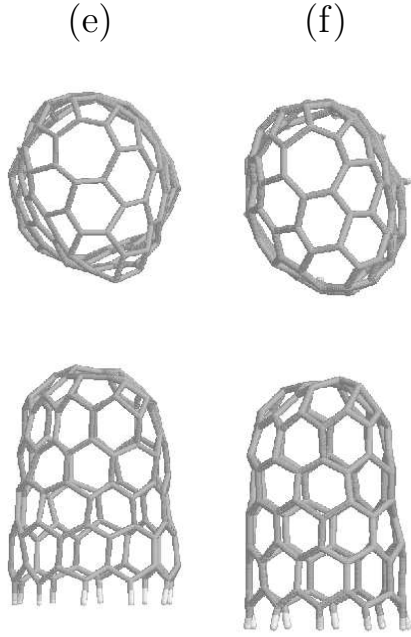


FIG. 3. Different stages of the closure of the (10,0) nanotube at 2500 K. These structures were observed at approximately (a) 2 ps, (b) 5 ps, (c) 8 ps, (d) 11 ps, (e) 15 ps and (f) 18 ps.

We now discuss the results obtained from the simulation of the (5,5) nanotube. During the first 10 ps of dynamics, in which the average temperature was fixed at 1000 K, one of the edges of a hexagon at the end of the nanotube is broken, and as a result a carbon chain is formed which oscillates under the influence of the thermal motion, but no (5/7) complexes are observed at this temperature. When the temperature is increased to 2000 K two more hexagons break, but still no (5/7) pairs are formed. At 2500 K nearly all edge hexagons have broken, and consequently there is an abundance of carbon chains. Among these the first two pentagons can be observed, but there are still no signs of heptagons. This is probably because the mechanism of pentagon formation in this case is somewhat different than in the (10,0) nanotube. In the latter, pentagons and heptagons occur in pairs, resulting from the fusion of two edge hexagons. Here the pentagons appear from the re-bonding of chains resulting from the breaking of edge hexagons. The presence of these pentagons induces curvature in the structure, which will eventually cause the tube closure. At 3000 K a total of three pentagons are seen, and the structure is rapidly evolving towards complete closure, but this only happens beyond 10 ps of dynamics at this temperature.

Our results show unambiguously that the open edges of nanotubes are unstable, and at sufficiently high temperatures close spontaneously by forming half-fullerene caps. The time scales we find for the nanotube closure are only orientative, as they may vary slightly for different initial conditions, and certainly they are sensitive to the temperature, but we can say that above 2000 K,

closure occurs within a few tens of ps. This finding is in agreement with previous first-principles results⁶². At temperatures between 1000 and 2000 K the time scale for closure (which remains beyond the scope of the simulation times covered here) could be in the order of hundreds of ps or even in the ns range, but even so this seems to us to be too short a time scale for permitting nanotube growth, and this is presumably why single-wall nanotubes cannot be obtained without using transition metal nano-particles which act as catalysts. However, the microscopic details of this catalytic growth process are as yet far from being understood⁶³.

In order to gain some insight into the experimental observation that boron doping can result in the production of longer and more crystalline multi-wall nanotubes, and in particular how it favors the zig-zag type tubes over the arm-chair or chiral ones, we have performed a number of static and dynamical simulations in the (10,0) nanotube system with different degrees of boron substitution.

B. Boron doped nanotubes

We first address the question as to why boron tends to accumulate at the ends of the nanotubes, as has been experimentally observed⁴⁸. To investigate this site preference, we have performed a series of relaxation calculations in which we compare the energy of nanotube and flat edge structures with a boron atom substituting a carbon atom at different sites. We have considered two different nanotube structures, one a zig-zag nanotube with indices (10,0) (the same as illustrated in Figure 1), and a (6,6) arm-chair nanotube. For each of the two structures we have taken into account five possible boron substitutional sites, namely: the boron atom substitutes at an edge carbon site (site α), the boron is located at a site one bond away from the edge site (site β), two bonds away (site γ), three (site δ) and six bonds away from the edge (site ϵ). These positions are illustrated schematically in Figure 4.

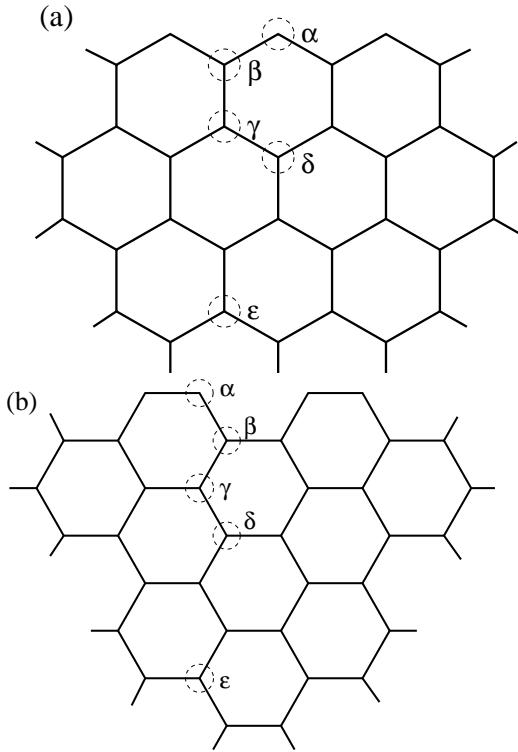


FIG. 4. (a) Schematic view of the boron substitutional sites considered in the (10,0) nanotube and the zig-zag graphene edge; (b) the substitutional sites in the (6,6) nanotube and arm-chair graphene edge.

Our results, given in Table I, show that in both types of nanotubes the most favorable position for boron to substitute at is in the vicinity of the edge. However, there are marked differences between both types of edges. In the zig-zag case, the energy of the structure with boron substituted in site β is 1.4 eV higher than the structure with boron substituted at the α site, almost the same as for substitution of boron far (site ϵ) from the edge (1.41 eV). So, in the case of the zig-zag edge it is much more favorable for boron to substitute at the edge than elsewhere in the nanotube. In the arm-chair edge, however, it turns out that the most stable structure is that in which the boron atom is placed at a site one bond away from the edge, i.e. site β in Figure 4(b), which turns out to be 0.58 eV more stable than the structure obtained by placing the boron atom directly at the edge (site α). Nevertheless, boron will still preferentially locate itself close to the edge rather than far away from it, as the energy difference between the most stable configuration and that with boron placed in site ϵ is 0.88 eV. These findings can be easily rationalized: in the zig-zag case it is more favorable for boron to be at the edge than elsewhere in the tube because in this way the number of carbon dangling bonds at the nanotube edge is reduced, given that boron has one electron less than carbon. In the arm-chair case, however, the same argument does not apply, because the carbon atoms at the edge are able to pair up forming a stable double bond. By placing a boron atom at the edge

a double bond cannot form, and the configuration that results is thus less stable than configuration β . The same trends are evident from the calculations involving the flat graphene edges, indicating that the curvature of the nanotubes does not play any significant part in determining the energetics of the boron-substituted structures.

TABLE I. Energies of boron-substituted structures for zig-zag and arm-chair nanotube and graphene edges. The energies are given in eV relative to the most stable structure in each case.

bonds from edge	(10,0) nanotube	zig-zag edge	(6,6) nanotube	arm-chair edge
0	0.00	0.00	0.58	0.48
1	1.39	0.99	0.00	0.00
2	0.57	0.67	0.60	0.66
3	1.30	1.42	0.83	0.75
6	1.41	1.35	0.88	0.88

These static calculations illustrate how boron could play a role in favoring zig-zag structures over arm-chair ones, as has been found experimentally. Our findings are in very good agreement with the DFT plane-wave pseudo-potential results reported by Blase and coworkers⁴⁸. However, these results do not give any explanation for the increased length of the nanotubes synthesized in the presence of boron. Thus, in order to gain some insight into how boron can assist the production of longer nanotubes, we have performed a series of MD simulations of a (10,0) nanotube with varying degrees of boron substitution at the edge. We have employed the same structure as illustrated in Figure 1, but placing four, six, eight and ten boron atoms at the tube edge, substituting as many carbon atoms in each case. Starting from such configurations, we have performed MD simulations following the same pattern described above for the undoped carbon nanotubes. Let us comment briefly on the details of the dynamics in each case. In all instances, at the lowest temperature considered (1000 K), the structures remain unaltered during the time spanned at this temperature (10 ps); all hexagonal rings present initially maintain their identity during this time, and it is not until the system is run at a temperature of 2000 K that structural changes begin to appear.

When only four boron atoms are present, after 10 ps of dynamics at 2000 K two (5/7) pairs are formed at the tube edge. The structure of these (5/7) pairs is such that the common edge between both rings always incorporates a boron atom [see Figure 5(a)]. This is a structural feature that repeats itself frequently in the other cases considered, as will be seen below. At this temperature, a transient C_4 ring, and a B_2C_6 octagonal ring are also seen. When the temperature is raised further to 2500 K, the boron containing pentagons still survive, but the heptagonal rings break, and carbon chains linked to the pentagons are formed. These chains, of length equal to two or three bonds, oscillate widely, eventually linking with similar chains or unsaturated bonds along the open edge, thus initiating the tube closure. The tube is closed after approximately 8.5 ps at this temperature. Given the low concentration of boron at the tip, the dynamics observed here is rather similar to that already described for the pure carbon case.

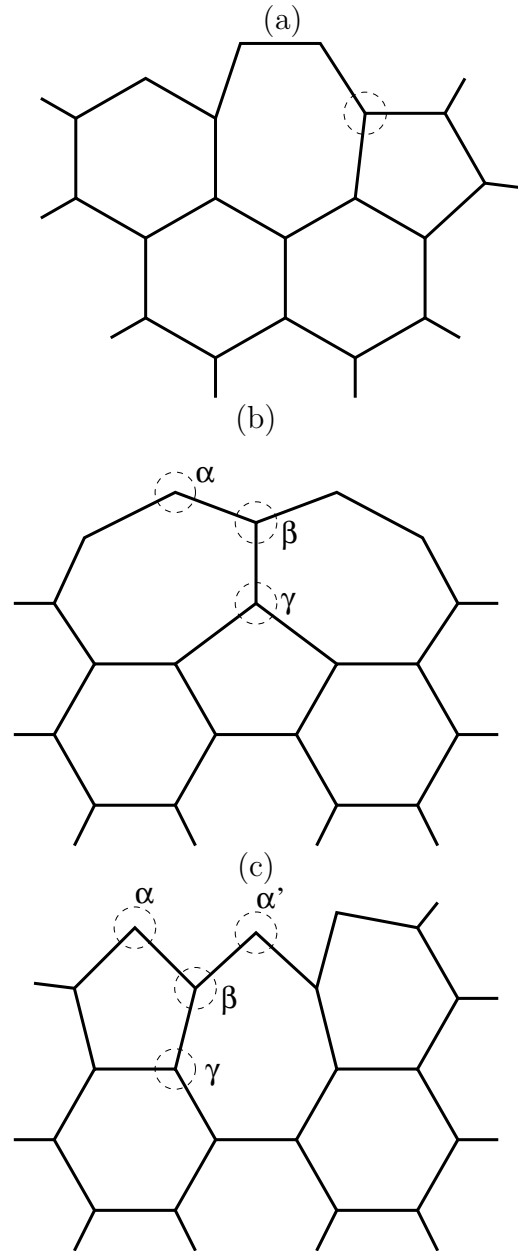


FIG. 5. Schematic view of (a) the (5/7) edge complex observed during the MD runs of the (10,0) nanotube (the circle indicates the position where boron is found in the boron doped cases); (b) one of the possible edge reconstructions involving pentagons and heptagons in the arm-chair type tubes, the (7/5/7) complex, and (c) the (5/7) arm-chair edge complex. The circles indicate the substitutional sites considered in the relaxation calculations (see text).

When the number of boron atoms is increased to 6, at the temperature of 2000 K two (5/7) complexes like those observed in the four-boron atom case are formed, but the structure is otherwise unaltered. These boron-containing (5/7) pairs are remarkably stable; they remain intact even after 10 ps at 2500 K. In this particular case, it is necessary to rise the temperature further, to 3000 K, for the tube closure to occur. This happens only after

8 ps of dynamics at this temperature, which is indicative of a higher stability of the open edge when compared to the tube with only four boron atoms. In the case of the nanotube doped with eight boron atoms, the structure develops two (5/7) pairs within 10 ps at 2000 K, much like in the previous cases. However, once the temperature is elevated to 2500 K, the structure closes completely within 7.5 ps. This result appears to contradict the thesis that increasing the amount of boron at the tube edge delays the closure process, but in fact this is not necessarily so, as will be argued below.

Finally, let us consider the case of the tube with ten boron atoms. Like in all the cases analyzed earlier, structural changes at the open edge begin to appear at a temperature of 2000 K, at which a boron-containing (5/7) pair is formed. Three such complexes can be seen after 10 ps at 2500 K, but the structure is otherwise unchanged. It is necessary to reach a temperature of 3000 K and monitor the dynamics of the system for 11 ps at this temperature before the tube can be said to be completely closed. We note that Blase and coworkers⁴⁸, who have also performed MD simulations of this particular system using DFT with a basis set of plane-waves and the pseudo-potential approximation up to temperatures of 2500 K for 10 ps, failed to observe the closure. The results reported here indicate that, at such a temperature, it is most likely that the closure would not occur below 10 ps, as it required 11 ps at 3000 K to observe the closure in the simulations that we have performed.

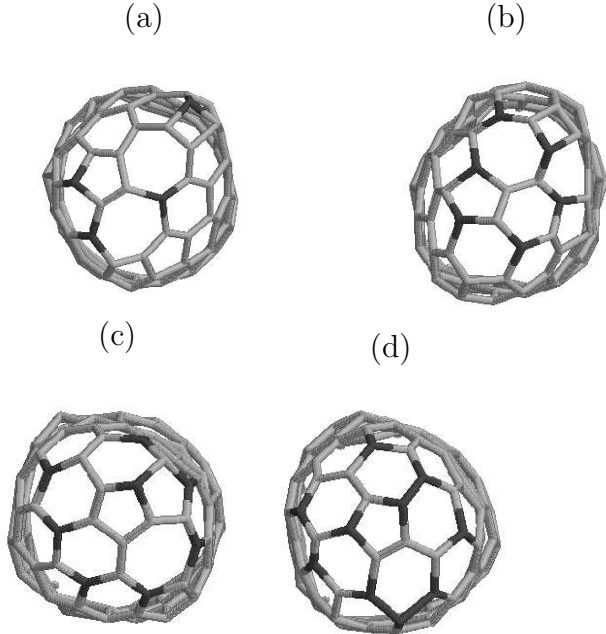


FIG. 6. The dome structures of the closed boron doped nanotubes arrived at during the MD simulations: (a) nanotube with four boron atoms, (b) nanotube with six boron atoms, (c) nanotube with eight boron atoms and (d) with ten boron atoms.

Figure 6 illustrates the structures obtained at the end of the MD simulations described above. As can be seen, regardless of the amount of boron present initially at the tube edge, the final structures are invariably closed, but as seen in the discussion, there are notable differences observed during the dynamics in each case. That the nanotubes evolve in such a way as to achieve a closed structure is, after all, not so surprising, given that the closed structures, with all atoms connected in an sp^2 network are always more stable than the corresponding open structures. For example, the structure illustrated in Figure 6(d), once relaxed at 0 K, is 13.7 eV more stable than the corresponding open structure (a figure to be compared with an energy difference of 17 eV, obtained for the pure carbon case using the same two structures). Nevertheless, as can be seen from the discussion above, the details of the closure process vary according to the amount of boron present at the edge.

Our MD results seem to indicate that a delay of the tube closure occurs when boron is present in the system. However, it is difficult to establish this beyond doubt purely on the basis of a small number of MD trajectories, because at each temperature and boron composition there will be a distribution of possible closure times (depending on the initial conditions) for a given type of nanotube. To get a clear picture of how the closure time distribution changes as the amount of boron is increased would require a very large sample of MD simulations, much larger than would be practical to carry out given the computational costs involved. Our simulations are clearly insufficient in number to reveal unambiguously the changing trends in closure times with increasing boron content, which could explain the apparently contradicting result obtained for the tube with eight boron atoms, which closes faster and at a lower temperature than the tube with only six boron atoms. Nevertheless, these simulations are sufficient to clarify the role played by boron when present at the open edge of a nanotube, and are thus extremely revealing. They indicate that before the tube closure can begin to occur, (5/7) complexes form at the edge. This is true of both the pure carbon and the boron doped tubes. Under the effect of the rapid thermal motion the heptagons seem to be more prone to breaking, and the chains of atoms thus formed initiate or can participate in the tube closure. Interestingly, when boron is present, it seems to be always associated with these structures once they are formed, in the manner depicted in Figure 5(a).

These observations have lead us to perform a new set of static structural relaxation calculations, in which we investigate the stability of these edge (5/7) complexes in both (n,0) and (n,n) nanotubes. We have compared the energy of a normal zig-zag edge structure, such as that shown in Figure 1 with that of a zig-zag edge containing a (5/7) pair, both in the pure carbon case and in the case in which the (5/7) pair contains a boron atom situated between the pentagon and heptagon at the edge [Figure 5(a)]. It turns out that a (5/7) pair placed at

the edge of a pure (10,0) tube lowers the total energy by about 0.56 eV. When boron is present between the pentagon and heptagon, the energy gain is slightly larger, 0.67 eV, according to our calculations. This seems to indicate that the formation of such boron containing edge complexes stabilizes the open edge, and consequently delays its closure.

A (5/7) complex is also possible at an arm-chair nanotube edge, where it is also possible to construct a more complicated edge structure, involving a pentagon and two heptagons, which we call a (7/5/7) edge complex; both structures are illustrated schematically in Figure 5(b) and 5(c). Structure 5(b) is reminiscent of the ring-defect structure discussed by Crespi *et al.*⁶⁴. We have investigated the stability of these, both in the pure carbon case and when boron is present in the different possible substitutional sites. The results from these calculations are listed in Table II. It turns out that the only reconstructed arm-chair edge which is more stable than the structure β shown in Figure 4(b) is that illustrated in Figure 5(b), with the boron atom placed between the two heptagonal rings, but not forming part of the pentagon (*i.e.* site β). Even so, the energy difference is only small (0.33 eV), certainly smaller than the energy gain obtained by the reconstruction in the zig-zag edge.

TABLE II. Energies of boron-substituted reconstructed edges for the (6,6) nanotube. The labeling of the edges corresponds to that of Figure 5 (b) and (c). The energies are given in eV relative to the most stable unreconstructed substituted arm-chair edge structure.

Position	Structure (b)	Structure (c)
α	1.10	3.40
β	-0.33	3.17
γ	0.46	2.67
α'	—	2.64

The results obtained from these structural relaxation calculations provide a possible mechanism for explaining both the observed preference for the zig-zag structure and the improved aspect ratio of nanotubes synthesized in the presence of boron. The reconstruction of a zig-zag edge in which boron is present from the saw-tooth structure illustrated in Figure 1 to one containing a (5/7) pair is exothermic, resulting in a significant stabilization of the nanotube. In the case of an undoped nanotube edge, this reconstruction also lowers the energy, but by a smaller amount. Note also that, while similar reconstructions are possible in the case of a boron doped arm-chair nanotube, only one such reconstructions lowers the energy with respect to the unreconstructed edge, and only by a small amount. Boron, thus, is seen to significantly stabilize zig-zag edges compared to arm-chair ones and we expect the former tubes to grow better; furthermore the edge (5/7) relaxation mechanism we have found is only effective in zig-zag edges, a fact that contributes to favor this type of tube even further.

IV. CONCLUSIONS

We have performed an extensive theoretical study of the effects of the presence of varying amounts of boron in the edge of growing nanotubes using TB MD and structural relaxation calculations. In spite of the approximate nature of the TB model used here, it gives results that compare quite well with the available FP data from the work of Blase *et al.*⁴⁸.

We have shown that both carbon and boron-doped nanotubes spontaneously close in a time scale of a few (≤ 20) ps in a temperature range of 2500-3000 K. In the case of boron-doped tubes the MD simulations reveal a pattern of longer closure times as the amount of boron at the tip of the nanotube is increased. The presence of boron in the proximity of the tube edge has a stabilizing effect, but this effect is larger in the case of zig-zag nanotubes than in the case of arm-chair ones. Furthermore, we have shown that in (n,0) edges a reconstruction of the edge involving (5/7) pairs stabilizes further the open edge. Although similar reconstructions are topologically possible in the case of (n,n) edges they do not result in any significant stabilization of this type of edge.

These results contribute to a better understanding of the experimental observations^{45,47,48} that boron accumulates at the nanotube tips, that it favors zig-zag nanotubes over other structures, and that the nanotubes synthesized in the presence of boron have a larger aspect ratio than other nanotubes.

* to whom correspondence should be addressed; email: ehe@icmab.es

ACKNOWLEDGMENTS

E.H. wishes to thank X. Blase, M. Terrones, N. Grobert, W.K. Hsu, H. Terrones and M.J. López for enlightening discussions. E.H. and P.O. thank the EU for financial support under project SATURN (IST-1999-10593). A.R. and J.A.A. acknowledge support by the DGES (Grant: PB98-0345), JCyL (Grant: VA28/99), and EU TMR NAMITECH project (ERBFMRX-CT96-0067 (DG12-MITH)). I.B. acknowledges support by the DGES (SAB 1995-0670P) of Spain during the sabbatical stay at the University of Valladolid, by the DFG (Deutsche Forschungsgemeinschaft Project SPP-Polyeder), and finally by the Fonds der Chemischen Industrie. We acknowledge the C⁴ (Centre de Computació i Comunicacions de Catalunya) and CEPBA (European Centre for Parallelism of Barcelona) for the use of their computer facilities.

-
- ¹ S. Iijima, *Nature* (London) **354**, 56 (1991).
 - ² M.S. Dresselhaus, G. Dresselhaus and P.C. Eklund, *Science of Fullerenes and Carbon Nanotubes* (Academic Press, New York 1996).
 - ³ T.W. Ebbesen (Ed.), *Carbon Nanotubes, Preparation and Properties* (CRC Press, Boca Raton 1997).
 - ⁴ P.M. Ajayan and T.W. Ebbesen, *Rep. Prog. Phys.* **60**, 1025 (1997).
 - ⁵ P.M. Ajayan, *Chem. Rev.* **99**, 1787 (1999).
 - ⁶ M. Terrones, W.K. Hsu, H.W. Kroto and D.R.M. Walton, *Topics in Current Chemistry* **199**, 189 (1999).
 - ⁷ M.M.J. Treacy, T.W. Ebbesen and J.M. Gibson, *Nature* (London) **381**, 678 (1996).
 - ⁸ N.G. Chopra and A. Zettl, *Solid State Comm.* **105**, 297 (1998).
 - ⁹ A. Krishnan, E. Dujardin, T.W. Ebbesen, P.N. Yanilos and M.M.J. Treacy, *Phys. Rev. B* **58**, 14013 (1998).
 - ¹⁰ E.W. Wong, P.E. Sheehan and C.M. Lieber, *Science* **277**, 1971 (1997).
 - ¹¹ E. Hernández, C. Goze, P. Bernier and A. Rubio, *Phys. Rev. Lett.* **80**, 4502 (1998).
 - ¹² J.P. Lu, *Phys. Rev. Lett.* **79**, 1297 (1997).
 - ¹³ B.I. Yakobson, C.J. Brabec and J. Bernholc, *Phys. Rev. Lett.* **76**, 2411 (1996).
 - ¹⁴ M. Buongiorno Nardelli, B.I. Yakobson and J. Bernholc, *Phys. Rev. B* **57**, R4277 (1998).
 - ¹⁵ N. Hamada, S. Sawada and A. Oshiyama, *Phys. Rev. Lett.* **68**, 1579 (1992).
 - ¹⁶ J.W.G. Wildöer, L.C. Venema, A.G. Rinzler, R.E. Smalley and C. Dekker, *Nature* (London) **391**, 59 (1998).
 - ¹⁷ J.P. Lu, *Phys. Rev. Lett.* **74**, 1123 (1995).
 - ¹⁸ W.H. Knechtel, G.S. Düsberg, W.J. Blau, E. Hernández and A. Rubio, *Appl. Phys. Lett.* **73**, 1961 (1998).
 - ¹⁹ P. Poncharal, Z.L. Wang, D. Ugarte and W.A. de Heer, *Science* **283**, 1513 (1999).
 - ²⁰ H. Dai, J.H. Hafner, A.G. Rinzler, D.T. Colbert and R.E. Smalley, *Nature* (London) **384**, 147 (1996).
 - ²¹ W.A. de Heer, A. Chatelain and D. Ugarte, *Science* **270**, 1179 (1995); A.G. Rinzler, J.H. Hafner, P. Nikolaev, L. Lou, S.G. Kim, D. Tománek, P. Norlander, D.T. Colbert and R.E. Smalley, *Science* **269**, 1550 (1995).
 - ²² P.G. Collins, A. Zettl, H. Bando, A. Thess and R.E. Smalley, *Science* **278**, 100 (1997).
 - ²³ S.J. Tans, A.R.M. Verschueren and C. Dekker, *Nature* (London), **393**, 49 (1998).
 - ²⁴ N.G. Chopra, R.J. Luyken, K. Cherrey, V.H. Crespi, M.L. Cohen, S.G. Louie and A. Zettl, *Science* **269**, 966 (1995).
 - ²⁵ A. Loiseau, F. Willaime, N. Demoncy, G. Hug and H. Pascard, *Phys. Rev. Lett.* **76**, 4737 (1996).
 - ²⁶ M. Terrones, W.K. Hsu, H. Terrones, J.P. Zhang, S. Ramos, J.P. Hare, R. Castillo, K. Prasides, A.K. Cheetham, H.W. Kroto and D.R.M. Walton, *Chem. Phys. Lett.* **259**, 568 (1996).
 - ²⁷ M. Terrones, A.M. Benito, C. Manteca-Diego, W.K. Hsu, O.I. Osman, J.P. Hare, D.G. Reid, H. Terrones, A.K. Cheetham, K. Prasides, H.W. Kroto and D.R.M. Walton, *Chem. Phys. Lett.* **257**, 576 (1996).
 - ²⁸ K. Suenaga, C. Colliex, N. Demoncy, A. Loiseau, H. Pascard and F. Willaime, *Science* **278**, 653 (1997).
 - ²⁹ L. Rapoport, Y. Bilik, Y. Feldman, M. Homyonfer, S.R. Cohen and R. Tenne, *Nature* (London) **387**, 791 (1997).
 - ³⁰ Y. Feldman, E. Wasserman, D.J. Srolovitz and R. Tenne, *Science* **267**, 222 (1995).
 - ³¹ R. Tenne, L. Margulis, M. Genut and G. Hodes, *Nature* (London) **360**, 444 (1992).
 - ³² Y.R. Hachohen, E. Grunbaum, R. Tenne, J. Sloan and J.L. Hutchinson, *Nature* (London) **395**, 336 (1998).
 - ³³ A. Rubio, J.L. Corkill and M.L. Cohen, *Phys. Rev. B* **49**, 5081 (1994).
 - ³⁴ X. Blase, A. Rubio, S.G. Louie and M.L. Cohen, *Europhys. Lett.* **28**, 335 (1994).
 - ³⁵ Y. Miyamoto, A. Rubio, S.G. Louie, and M.L. Cohen, *Phys. Rev. B* **50**, 18360 (1994).
 - ³⁶ Y. Miyamoto, A. Rubio, S.G. Louie, and M.L. Cohen, *Phys. Rev. B* **50**, 4976 (1994).
 - ³⁷ S.M. Lee, Y.H. Lee, Y.G. Hwang, J. Elsner, D. Porezag and Th. Frauenheim, *Phys. Rev. B* **60**, 7788 (1999).
 - ³⁸ I. Boustani, A. Quandt, E. Hernández and A. Rubio, *J. Chem. Phys.* **110**, 3176 (1999).
 - ³⁹ M. Cote, M.L. Cohen and D.J. Chadi, *Phys. Rev. B* **58**, 4277 (1998).
 - ⁴⁰ G. Seifert and E. Hernández, *Chem. Phys. Lett.* **318**, 355 (2000).
 - ⁴¹ M.R. Ghadiri, J.R. Granja, R.A. Milligan, D.E. McRee and N. Khazanovich, *Nature* (London) **366**, 324 (1993).
 - ⁴² P. Carloni, W. Andreoni and M. Parrinello, *Phys. Rev. Lett.* **79**, 761 (1997).
 - ⁴³ A. Thess, R. Lee, P. Nikolaev, H. Dai, P. Petit, J. Robert, C. Xu, Y.H. Lee, S.G. Kim, A.G. Rinzler, D.T. Colbert, G.E. Scuseria, D. Tománek, J.E. Fischer and R.E. Smalley, *Science* **273**, 483 (1996).
 - ⁴⁴ S. Bandow, S. Asaka, Y. Saito, A.M. Rao, L. Grigorian, E. Richter and P.C. Eklund, *Phys. Rev. Lett.* **80**, 3779

- (1998).
- ⁴⁵ P. Redlich, J. Loeffler, P.M. Ajayan, J. Bill, F. Aldinger and M. Ruhle, Chem. Phys. Lett. **260**, 465 (1996).
 - ⁴⁶ D.L. Carroll, P. Redlich, P.M. Ajayan, S. Curran, S. Roth and M. Ruhle, Carbon **36**, 753 (1998).
 - ⁴⁷ M. Terrones, W.K. Hsu, A. Schilder, H. Terrones, N. Grobert, J.P. Hare, Y.Q. Zhu, M. Schwoerer, K. Prasad, H.W. Kroto and D.R.M. Walton, Appl. Phys. A **66**, 307 (1998).
 - ⁴⁸ X. Blase, J.-C. Charlier, A. de Vita, R. Car, P. Redlich, M. Terrones, W.K. Hsu, H. Terrones, D.L. Carroll and P.M. Ajayan, Phys. Rev. Lett. **83**, 5078 (1999).
 - ⁴⁹ For a review on tight-binding see C.M. Goringe, D.R. Bowler and E. Hernández, Rep. Prog. Phys. **60**, 1447 (1997).
 - ⁵⁰ D. Porezag, T. Frauenheim, T. Köhler, G. Seifert and R. Kashner, Phys. Rev. B **51**, 12947 (1995).
 - ⁵¹ J. Widany, T. Frauenheim, T. Köhler, M. Sternberg, D. Porezag, G. Jungnickel and G. Seifert, Phys. Rev. B **53**, 4443 (1996).
 - ⁵² P.W. Fowler, T. Heine, D. Mitchell, G. Orlandi, R. Schmidt, G. Seifert and F. Zerbetto, J. Chem. Soc., Faraday Trans. **92**, 2203 (1996).
 - ⁵³ A. Ayuela, P.W. Fowler, D. Mitchell, R. Schmidt, G. Seifert and F. Zerbetto, J. Phys. Chem. **100**, 15634 (1996).
 - ⁵⁴ H. Terrones, M. Terrones, E. Hernández, N. Grobert, J.-C. Charlier and P.M. Ajayan, Phys. Rev. Lett. **84**, 1716 (2000).
 - ⁵⁵ F. Fugaciu, H. Hermann and G. Seifert, Phys. Rev. B **60**, 10711 (1999).
 - ⁵⁶ W.H. Press, S.A. Teukolsky, W.T. Vetterling and B.P. Flannery, *Numerical Recipes, the Art of Scientific Computing* 2nd Edition (Cambridge University Press 1992).
 - ⁵⁷ S. Nosé, J. Chem. Phys. **81**, 511 (1984).
 - ⁵⁸ W.G. Hoover, Phys. Rev. A **31**, 1695 (1985).
 - ⁵⁹ D. Frenkel and B. Smit, *Understanding Molecular Simulation*, Academic Press, San Diego (1996).
 - ⁶⁰ A.J. Stone and D.J. Wales, Chem. Phys. Lett. **128**, 501 (1986).
 - ⁶¹ T.R. Welsh and D.J. Wales, J. Chem. Phys. **109**, 6691 (1998).
 - ⁶² J.-C. Charlier, A. De Vita, X. Blase, and R. Car, Science **275**, 646 (1997).
 - ⁶³ H. Kanzow and A. Ding, Phys. Rev. B **60**, 11180 (1999).
 - ⁶⁴ V.H. Crespi, M.L. Cohen and A. Rubio, Phys. Rev. Lett. **79**, 2093 (1997).